Tight focusing with a binary microaxicon

V. V. Kotlyar,[1] S. S. Stafeev,[2,*] L. O'Faolain,[3] and V. A. Soifer[2]

[1]Image Processing Systems Institute of the Russian Academy of Sciences, 151 Molodogvardeyskaya Street, Samara 443001, Russia

[2]S. P. Korolyov Samara State Aerospace University (National Research University), 34 Moskovskoe Street, Samara 443086, Russia

[3]SUPA, School of Physics and Astronomy of the University of St. Andrews, North Haugh, St. Andrews, KY16 9SS, Scotland, UK

*Corresponding author: sergey.stafeev@gmail.com

Received April 26, 2011; revised July 7, 2011; accepted July 7, 2011; posted July 11, 2011 (Doc. ID 146619); published August 8, 2011

Using a near-field scanning microscope (NT-MDT) with a 100 nm aperture cantilever held 1 μm apart from a microaxicon of diameter 14 μm and period 800 nm, we measure a focal spot resulting from the illumination by a linearly polarized laser light of wavelength $\lambda = 532$ nm, with its FWHM being equal to 0.58λ, and the depth of focus being 5.6λ. The rms deviation of the focal spot intensity from the calculated value is 6%. The focus intensity is five times larger than the maximal illumination beam intensity.

OCIS codes: 050.1380, 180.4243.

Axicons are known to be suitable for generating a diffraction-free laser Bessel beam at a certain optical axis segment. Despite being widely known in optics for quite some time, interest in axicons has not weakened. Surface plasmons with a sharp central peak were generated in metal films by use of an axicon in Refs. [1,2]. A binary axicon of period 33 μm was studied in Ref. [3]. The minimal diameter of the laser beam was 1.2 μm (at wavelength $\lambda = 532$ nm). The laser beam diameter was shown to be independent of the wavelength. In Ref. [4], an axicon made of glass with the vertex angle of 175° was employed as a wavefront sensor, whereas Ref. [5] reported on the generation of an annular collimated laser beam of diameter 8 mm with the aid of two axicon mirrors. A diffractive axicon of diameter 2 mm and period 20 μm was investigated using a Mach–Zehnder interferometer in Ref. [6]. Fabrication of a microaxicave (inverted microaxicon) of period 20 μm to generate a ring of radius 1.5 mm at a distance of 50 mm was reported in Ref. [7].

To the best of our knowledge, Ref. [8] is the only publication where the use of the axicon for the tight focusing of laser light was reported. In Ref. [8] a radially polarized Bessel beam formed by passing an Ar laser beam (wavelength $\lambda = 514$ nm) through an axicon with NA = 0.67 was registered in a PMMA-DR1 (polymer matrix PMMA with azobenzene molecules) layer, which selectively registered the longitudinal E-vector component. The Bessel beam diameter was experimentally measured to be FWHM = 0.62λ In a similar way, a circularly polarized Bessel beam of diameter FWHM = 0.60λ was registered in the PMMA-DR1 medium. It is noteworthy that without a special registration medium, PMMA-DR1, the beam diameter would have been FWHM = 0.89λ.

In a number of papers [9–12], the focus depth was reported to be increased using axiconlike binary phase diffractive elements (DOEs) with their radius jumps fitted in a special manner. Thus, in [9,10] by modeling based on Richards and Wolf formulas, a four-ring DOE matched to a lens with NA = 0.95 was shown to form a focal segment of diameter FWHM = 0.43λ and depth DOF = 4λ. The DOE was illuminated with a radially polarized Bessel–Gaussian beam. In similar modeling reported in [11], a lens with spherical aberration (lens axicon) was employed. In this way, it became possible to obtain the best characteristics of the focal line, namely, FWHM = 0.395λ and DOF = 6λ. In Ref. [12], using a radially polarized Bessel–Gaussian beam bounded with a narrow annular aperture and a microlens (NA = 0.9), a focal spot of diameter FWHM = 0.61λ was experimentally obtained (although the simulated value was as small as FWHM = 0.4λ). Note that all these articles [9–12] treat the far-field focusing (in the lens focus).

In this Letter, we study the tight focusing by a binary microaxicon of diameter 14 μm, period 800 nm, microrelief depth 465 nm, and NA = 0.665. Using a near-field scanning microscope, with a 100-nm-aperture cantilever positioned 1 μm apart from the axicon surface, we measured the intensity distribution in the focal spot produced by linearly polarized laser light ($\lambda = 532$ nm). The focal spot diameter was measured to be FWHM = 0.58λ, with the focal depth being DOF = 5.6λ. The rms deviation of the intensity distribution in the focal spot from the calculated value was 6%. The resulting focal intensity was five times higher than the illumination beam maximal intensity. Note that the measured value of diameter (0.58λ) was smaller than that reported in Ref. [12] (0.61λ), whereas the axicon's NA (0.67) was smaller than that of the lens (0.9) in Ref. [12].

A high-quality binary axicon was fabricated using electron beam lithography. A thin layer of ZEP520A resist coated on a glass substrate was then exposed to 180 °C heat for 10 min in order to drive off the solvent. The resist thickness was carefully controlled so that it would be sufficient to ensure the required phase shift of the axicon. The pattern of concentric rings was written in the resist with an electron beam using the electron microscope Zeiss GEMINI (Carl Zeiss AG, Germany) with a lithographic device Raith ELPHY Plus (Raith GmbH, Germany) at voltage 30 kV. The pixel size was 10 nm, the exposure energy being 45 mAc/cm^2. Following the exposure, the sample was developed in xylene at 23 °C and then rinsed in isopropanol. The remaining resist formed an axicon of period 800 nm (the resist refractive index $n = 1.5$). Figure 1 presents an electron image of the axicon under characterization, the profile height being 465 nm. From Fig. 1, the binary microrelief height is seen to be approximately equal to one reading (500 nm) of the scale shown on the right bottom. For clarity, Fig. 1(c) depicts an optical arrangement with the axicon and the incident Gaussian beam in the Cartesian coordinates.

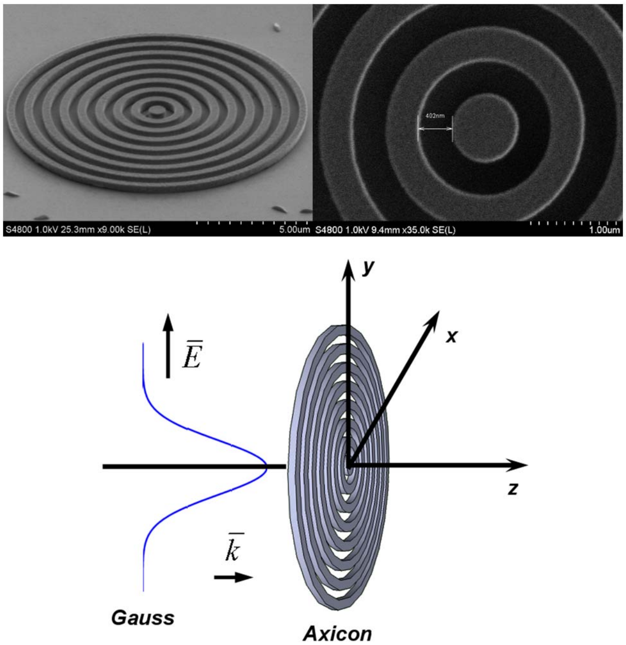

Fig. 1. (Color online) A scanning electron microscope image of a binary axicon of period 800 nm: (a) tilted view, (b) top view (enlarged), and (c) an optical arrangement containing the axicon and the Gaussian beam.

Using the near-field scanning microscope NT-MDT, we studied the passage of a linearly polarized Gaussian beam (radius 7λ) of wavelength $\lambda = 0.532\,\mu$m through the aforesaid binary axicon of period 800 nm. Figure 2(a) shows an enlarged image of a cantilever with a 100 nm aperture, which was utilized for the measurements. The aperture in Fig. 2(a) is shown as a horizontal white segment. The near-field intensity distribution was measured in the following manner. Linearly polarized light from a solid-state laser L with wavelength 532 nm was focused by the lens L1 onto the surface of a glass substrate with a microaxicon, A1, located in it. Passing through the substrate, the light was diffracted by the axicon. A cantilever with aperture, C1, found immediately behind the axicon, conducted the parallel scanning of the axicon surface at different distances from it. Having passed through the cantilever aperture, the light was then focused by the lens L2, transmitted through the spectrometer S (to filter off the irrelevant light), and registered by the CCD camera.

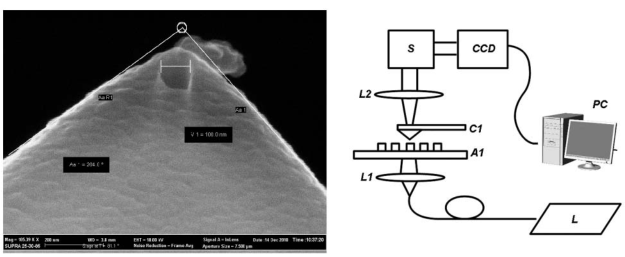

Fig. 2. (a) Shape of a four-sided cantilever with a 100 nm aperture (shown as a horizontal white segment) that was used in the near-field microscope NT-MDT and (b) an experimental optical schematic: L, laser; L1, L2, lenses; A1, axicon under study on the substrate; C1, cantilever with an aperture; S, spectrometer; CCD, camera; PC, computer.

Figure 3 illustrates an example of the intensity distribution measured with the microscope NT-MDT [Fig. 2(b)] $1\,\mu$m from the axicon surface. The spot diameter was FWHM $= 0.58\lambda$. The intensity in Fig. 3(b) (curve 2) is presented in relative units. Note that the focal intensity was found to be five times higher than the maximal intensity of the illumination Gaussian beam. This was attained by shifting the axicon on the substrate A1 [Fig. 2(b)] across the optical axis by $20\,\mu$m, so that the incident beam would only pass through the substrate, and repeatedly measuring the intensity. The conversion efficiency was as low as 6%. This is because the contribution to the focal spot [Fig. 3(a)] came only from the first circle and ring of the axicon relief [Fig. 1(b)]. This conversion efficiency is lower than that reported in Refs. [9] (20%, DOF $= 4\lambda$) and [11] (15%, DOF $= 6\lambda$). Note, however, that in [9,11] it was only the theoretical efficiency that was considered.

A comparison between the experimental intensity distribution in the focus (formed $1\,\mu$m from the axicon surface along the optical axis z) and the simulated intensity distribution is depicted in Fig. 3(b). The simulation was conducted using a radial finite-difference time-domain method with the code written in MATLAB [13].

The rms deviation of the curves in Fig. 3(b) is 6%. Note that major differences between the curves in Fig. 3(b) are to be found in the side lobes of the diffraction pattern, whereas the deviation of the major intensity peak at $|x| \le 1\,\mu$m from the simulated value is as small as 1%. A noticeable increase in the side lobes in comparison with the theoretical estimation is due to the fact that, among other factors, the amplitude of the signal that comes from the cantilever depends on its distance from the surface (on the local relief shape). Figure 4 shows the simulated intensity distribution along the optical axis z. The vertical line in Fig. 4 marks the axicon surface. Experimental values of the intensity in Fig. 4 are marked as squares crossed with vertical lines, with the lines denoting the admissible magnitude of the intensity measurement error. The longitudinal depth of the axicon focus at half-maximum is DOF $= 3\,\mu\text{m} = 5.6\lambda$ (Fig. 4).

It is a well known fact that an axicon forms a Bessel beam, with the Bessel beam diameter derived from the expression $J_0{}^2(kr\sin\theta) = 0$. In Ref. [14] the above formula was shown to define the smallest possible spot for any vector field. Although, strictly speaking, it should be noted that for the linearly polarized beam, the contribution to the focal spot comes from three Bessel functions, J_0, J_1, and J_2 [15]. Thus, we find that the beam diameter

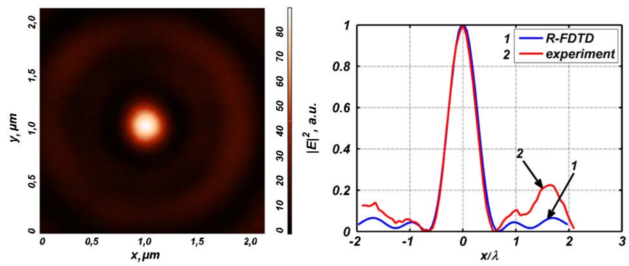

Fig. 3. (Color online) (a) Near-field scanning optical microscope image of the intensity distribution in the spot and (b) intensity profile along the x axis: simulation (curve 1) and experiment (curve 2).

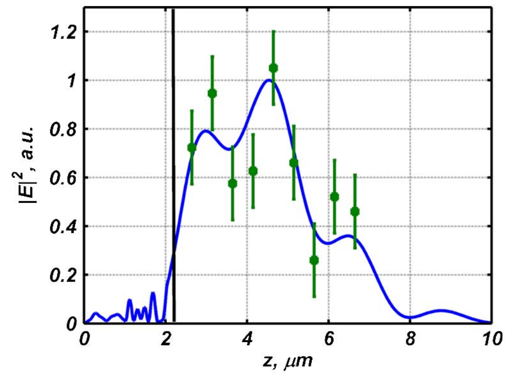

Fig. 4. (Color online) Longitudinal intensity profile along the optical axis: experiment (marked as squares with vertical lines) and simulation (curve).

is $2r = 2.4\lambda/(n \sin\theta)$, where θ is the half-angle at the vertex of a conical wave formed by the axicon. If the binary axicon is interpreted as a diffraction grating [3], the angle θ of the conical wave simultaneously represents the diffraction order angle for a grating of period T: $\sin\theta_m = m\lambda/T$, where m is the diffraction order number. The final expression for evaluating the diameter of the axicon light field on the optical axis can be obtained in the form $2r = 2.4\,T/(m\Pi) = 0.774\,T/m$. This expression suggests that, for the binary axicon, the Bessel beam diameter is independent of the illumination wavelength [3], being only determined by the axicon period and the diffraction order number. Let us evaluate the diameter of a focal spot produced by our binary microaxicon of period $T = 800\,\mathrm{nm}$ ($\mathrm{NA} = \lambda/T = 0.665$ at $m = 1$): $\mathrm{FWHM} = 0.36\lambda/\mathrm{NA} = 0.54\lambda$ (according to Ref. [14], this is the smallest possible value at a given NA). Thus, the experimentally derived value of the focal spot diameter ($\mathrm{FWHM} = 0,58\lambda$) differs from the theoretical estimate ($\mathrm{FWHM} = 0,54\lambda$) by as little as 8%. The larger value of the focal spot size (0.89λ) reported in Ref. [8] for a similar axicon ($\mathrm{NA} = 0.67$) can be ascribed to the use of the near-field microscope with the bare fiber sharp tip. It can be conjectured that the dielectric tip increases the focus diameter to a greater extent than the metal cantilever with a pinhole, which was utilized in this work.

Summing up, the following results have been derived. By e-beam lithography on ZEP520A resist, a binary microaxicon of diameter $14\,\mu\mathrm{m}$, period $800\,\mathrm{nm}$, and relief depth $465\,\mathrm{nm}$ has been fabricated. Using a near-field scanning microscope NT-MDT with a 100-nm-aperture cantilever positioned $1\,\mu\mathrm{m}$ from the axicon surface, we have registered a focal spot produced by a linearly polarized laser light of wavelength $532\,\mathrm{nm}$ with diameter at half-maximum equal to $\mathrm{FWHM} = 308\,\mathrm{nm}$, which amounts to 0.58λ. The average deviation of the experimental intensity in focus from the simulated value is not larger than 6%. The experimentally derived value of the focal spot diameter differs from the theoretical estimate ($\mathrm{FWHM} = 0,54\lambda$) by as little as 8%. The focus depth at half-maximum is $\mathrm{DOF} = 5.6\lambda$. The intensity maximum on the optical axis has been found to be five times larger than the illumination beam intensity.

Such types of generated beams have many important potential applications in optical manipulations [16], optical microscopy [15,17], and particle acceleration [18].

The fabrication was carried out in the framework of NanoPix [19].

The work was financially supported by the Federal target program "Research and Academic Staff of Innovative Russia" (contract 14.740.11.0016) and the RF Presidential Grant for Support of Leading Scientific Schools (NSh-7414.2010.9). L. O'Faolain was supported by the Era-NET NanoSci LECSIN project.

References

1. W. Chen and Q. Zhan, Opt. Lett. **34**, 722 (2009).
2. K. Watanabe, G. Terakedo, and H. Kano, Opt. Lett. **34**, 1180 (2009).
3. Y. Kizuka, M. Yamauchi, and Y. Matsuoka, Opt. Eng. **47**, 053401 (2008).
4. B. Vohnsen, S. Castillo, and D. Rativa, Opt. Lett. **36**, 846 (2011).
5. S. K. Tiwari, S. R. Mishra, and S. P. Ram, Opt. Eng. **50**, 014001 (2011).
6. D. Kuang, M. Han, H. Gao, Z. Du, and Z. Fang, J. Opt. **13**, 035501 (2011).
7. D. Kuang and Z. Fang, Opt. Lett. **35**, 2158 (2010).
8. T. Grosjean, D. Courjon, and C. Bainier, Opt. Lett. **32**, 976 (2007).
9. H. Wang, L. Shi, B. Lukyanchuk, C. Sheppard, and C. T. Chong, Nat. Photon. **2**, 501 (2008).
10. K. Huang, P. Shi, X. Kang, X. Zhang, and Y. Li, Opt. Lett. **35**, 965 (2010).
11. K. B. Rajesh, Z. Jaroszewicz, and P. M. Anbarasan, Opt. Express **18**, 26799 (2010).
12. K. Kitamura, K. Sakai, and S. Noda, Opt. Express **18**, 4518 (2010).
13. V. V. Kotlyar and S. S. Stafeev, Opt. Commun. **282**, 459 (2009).
14. T. Grosjean and D. Courjon, Opt. Commun. **272**, 314 (2007).
15. E. J. Botcherby, R. Juskaitis, and T. Wilson, Opt. Commun. **268**, 253 (2006).
16. K. Dholakia and T. Cizmar, Nat. Photon. **5**, 335 (2011).
17. L. Liu, C. Liu, W. C. Howe, C. J. R. Sheppard, and N. Chen, Opt. Lett. **32**, 2375 (2007).
18. R. D. Romea and W. D. Kimura, Phys. Rev. D **42**, 1807 (1990).
19. URL: http://www.nanophotonics.eu.